Original Article

MOLECULAR METABOLISM

Adipocyte CAMK2 deficiency improves obesity-associated glucose intolerance

Wen Dai [1,2], **Mayank Choubey** [1], **Sonal Patel** [1], **Harold A. Singer** [3], **Lale Ozcan** [1,*]

ABSTRACT

Objective: Obesity-related adipose tissue dysfunction has been linked to the development of insulin resistance, type 2 diabetes, and cardiovascular disease. Impaired calcium homeostasis is associated with altered adipose tissue metabolism; however, the molecular mechanisms that link disrupted calcium signaling to metabolic regulation are largely unknown. Here, we investigated the contribution of a calcium-sensing enzyme, calcium/calmodulin-dependent protein kinase II (CAMK2), to adipocyte function, obesity-associated insulin resistance, and glucose intolerance.
Methods: To determine the impact of adipocyte CAMK2 deficiency on metabolic regulation, we generated a conditional knockout mouse model and acutely deleted CAMK2 in mature adipocytes. We further used *in vitro* differentiated adipocytes to dissect the mechanisms by which CAMK2 regulates adipocyte function.
Results: CAMK2 activity was increased in obese adipose tissue, and depletion of adipocyte CAMK2 in adult mice improved glucose intolerance and insulin resistance without an effect on body weight. Mechanistically, we found that activation of CAMK2 disrupted adipocyte insulin signaling and lowered the amount of insulin receptor. Further, our results revealed that CAMK2 contributed to adipocyte lipolysis, tumor necrosis factor alpha (TNFα)—induced inflammation, and insulin resistance.
Conclusions: These results identify a new link between adipocyte CAMK2 activity, metabolic regulation, and whole-body glucose homeostasis.

Keywords CAMK2; Adipose tissue; Obesity; Glucose intolerance; Insulin resistance; Insulin signaling; Lipolysis; Adipocyte inflammation

1. INTRODUCTION

Adipose tissue is now accepted as an important endocrine organ that contributes to whole-body energy homeostasis. White adipose tissue (WAT) stores lipids and secretes hormones and cytokines, including leptin, adiponectin, and tumor necrosis factor alpha (TNFα), whereas brown adipose tissue (BAT) generates heat and contributes to energy homeostasis [1]. During periods of energy excess or feeding, activation of adipocyte insulin signaling results in glucose uptake, lipogenesis, inhibition of lipolysis, and triglyceride storage. Obesity-induced impairment of WAT insulin signaling and the resultant lipolysis lead to ectopic lipid deposition in metabolically-active organs, such as liver and skeletal muscle [2]. Furthermore, lipolysis-driven macrophage infiltration of WAT, which initially serves an adaptive role in metabolizing excess free fatty acids (FFA), becomes maladaptive in obesity, and the resultant chronic inflammation further promotes the progression of insulin resistance [3,4]. Although much is known about the regulation of adipocyte insulin receptor (INSR) signaling under physiologic conditions, there are still gaps in our understanding of the upstream signaling pathways that contribute to altered adipose tissue insulin sensitivity in obesity. Identifying factors that regulate WAT function may reveal therapeutic strategies for insulin resistance and type 2 diabetes mellitus (T2D).

The role of calcium homeostasis in metabolic disturbances has become a topic of interest in recent years. Although changes in intracellular calcium levels and calcium-dependent signaling events have been well-studied in the regulation of hepatic glucose metabolism, their roles in adipocyte function are largely unknown. Studies in isolated human adipocytes revealed increased intracellular calcium concentrations and a concomitant reduction in glucose uptake in obese subjects [5]. In drosophila, store-operated calcium entry regulator, stromal interaction molecule 1 (STIM1) and the endoplasmic reticulum—localized calcium channel, inositol triphosphate receptor (ITPR) have been implicated in regulating adiposity and lipid metabolism [6,7], yet molecular mediators of this regulation have not been studied. We and others have previously reported that a calcium-sensitive kinase, calcium/calmodulin dependent-protein kinase II (CAMK2), becomes activated in liver during fasting and obesity and plays a critical role in glucose homeostasis [8—13]. Deletion or inhibition of hepatic CAMK2 in obese mice protects against glucose intolerance and hyperinsulinemia [9,14]. The mechanism of metabolic benefit through CAMK2 inhibition involves suppression of gluconeogenesis and improvement in hepatic insulin signaling. However, the role of CAMK2 in other insulin-sensitive tissues, including WAT, is still unknown.
Here, we report that CAMK2 is activated in obese adipose tissue, which in turn plays a role in metabolic dysfunction. Using cultured

[1]Department of Medicine, Columbia University Irving Medical Center, New York, NY, USA [2]Department of Cardiology, The Second Xiangya Hospital, Central South University, Changsha, China [3]Department of Molecular and Cellular Physiology, Albany Medical College, Albany, NY, USA

*Corresponding author. 630 West 168th Street, Black Building: 901D, New York, NY, 10032, USA. Fax: +12123055052. E-mail: lo2192@cumc.columbia.edu (L. Ozcan).

Received June 25, 2021 • Accepted July 13, 2021 • Available online 22 July 2021

https://doi.org/10.1016/j.molmet.2021.101300

adipocytes deficient in CAMK2 and an inducible mouse model of CAMK2 deficiency in adipose tissue, we report that adipocyte CAMK2 regulates insulin signaling and whole-body glucose homeostasis. Moreover, we provide evidence that CAMK2 is involved in adipocyte lipolysis and inflammation, which may further contribute to the pathogenesis of insulin resistance. Taken together, these data identify adipocyte CAMK2 as a critical component of metabolic regulation in obesity.

2. MATERIALS AND METHODS

2.1. Mice

Floxed *Camk2d/g* mice were generated by crossbreeding *Camk2d*$^{loxP/loxP}$ and *Camk2g*$^{loxP/loxP}$ mice as described previously [15,16], then crossing them onto the C57BL6/J background. These mice were then bred with mice expressing a tamoxifen-inducible Cre recombinase under the control of the *Adipoq* gene promoter (Jax mice, 025124) to generate adipocyte-inducible CAMK2δ and CAMK2γ double knockout mice (Ai-CAMK2 KO). Littermate mice carrying the floxed alleles served as controls. For all experiments, male mice of the same age and similar weight were randomly assigned to experimental and control groups. Mice were fed a high-fat diet (HFD) with 60% kcal from fat (Research Diets, D12492) immediately after weaning and maintained on a 12-hr light–dark cycle. Two separate cohorts of Ai-CAMK2 KO and control mice that were fed with HFD for a total of 7 and 20 weeks, respectively, were treated with 75 mg/kg tamoxifen (Cayman, 13528) dissolved in 10% ethanol and 90% corn oil (Sigma) i.p. for five consecutive days. Mice were maintained on HFD and experiments were commenced 2–10 weeks after tamoxifen treatment. Total HFD feeding period was 15 and 30 weeks, respectively. Additionally, *Camk2d*$^{loxP/loxP}$ and *Camk2g*$^{loxP/loxP}$ mice were bred with *Adipoq-Cre*–transgenic mice (Jax mice, 028020), which express Cre in a non-inducible manner (A-CAMK2 KO), and fed with HFD for 16 weeks. A glucose meter was used to measure blood glucose in mice that were fasted overnight (with free access to water). Plasma insulin levels were measured using an ultrasensitive mouse insulin ELISA Kit (Crystal Chem). The homeostasis model assessment of insulin resistance (HOMA-IR) index was calculated using the following formula: fasting plasma insulin (in mU/l) × fasting blood glucose (in mMol/l)/22.5 [17,18]. Enzymatic assay kits were used to measure plasma total cholesterol (Wako Diagnostics), triglycerides (Wako Diagnostics), non-esterified fatty acids (NEFA, Wako Diagnostics), glycerol (Sigma), and β-hydroxybutyrate (Abcam). Glucose tolerance tests (GTTs) were performed in overnight-fasted mice by assaying blood glucose at various times after i.p. injection of glucose (1–1.5 g/kg). Insulin tolerance tests (ITTs) were performed in 5-hr–fasted mice by assaying blood glucose at various times after i.p. injection of insulin (0.6–1 IU/kg). Diet-induced obese mice (Jax mice, 380050), their respective controls (Jax mice, 380056), and *ob/ob* mice (Jax mice, 000632) were used for the analysis of CAMK2 phosphorylation in WAT and BAT. Animal studies were performed in accordance with the Columbia University Irving Medical Center Institutional Animal Care and Use Committee.

2.2. Portal vein insulin infusion

Following 5-hr food withdrawal, mice were anesthetized and insulin (0.6 IU/kg) or PBS was injected through the portal vein. Three minutes after injection, tissues were removed, frozen in liquid nitrogen, and kept at −80 °C until processing.

2.3. Reagents and antibodies

Insulin, sodium palmitate, polybrene, cycloheximide, isoproterenol, chloroquine, ammonium chloride, MG132, chlorpromazine, filipin, KN93 (CAS# 139298-40-1), and KN92 (CAS# 1135280-28-2) were from Sigma. TNFα was from Peprotech. Anti-phospho-S473-AKT, anti-AKT, anti-phospho-Y1150/1151-INSR, anti-INSR, anti-HSP90, anti-phospho-T183/Y185-JNK, anti-JNK, anti-β-ACTIN, and anti-pan CDH antibodies were from Cell Signaling Technology. Anti-phospho-T287-CAMK2 antibody was from Novus, anti-CAMK2δ antibody was from Genetex, anti-CAMK2γ antibody was from Santa Cruz Biotech, and anti-transferrin receptor 1 (TFRC1) antibody was from Thermo. Adenoviruses encoding LacZ and CA-CAMK2 were described previously [19] and amplified by Viraquest, Inc. (North Liberty, IA).

2.4. Cell culture experiments

OP9 cells (ATCC, CRL-2749) were maintained in media containing MEMα, 20% (v/v) heat-inactivated FBS, and 1X penicillin-streptomycin. To induce differentiation, cells were incubated in media containing MEMα, 15% (v/v) KnockOut™ serum replacement (SR, Invitrogen, 10828–028), and 1% penicillin-streptomycin for 4 days. The medium was then changed to MEMα, 20% (v/v) heat-inactivated FBS, and 1% penicillin-streptomycin, and the cells were cultured for 2 more days. Differentiated cells were transfected with scrambled RNA or siRNAs targeting *Camk2d* (Integrated DNA Technologies, predesigned dsiRNA, target sequence: 5′-AGCCAAGAGUUUAUUGAA-3′ and 3′-CGUCGGUUCUCAAAUAACUUCUUUGGU-5′) and *Camk2g* (Qiagen, predesigned siRNA, target sequence: 5′-ACAGTCACTCCTGAAGCTAA-3′) using Lipofectamine RNAiMAX transfection reagent (Life Technologies, Inc.) according to the manufacturer's instructions. Transduction with adenoviruses encoding LacZ or CA-CAMK2 were carried out using polybrene (2 ug/mL). In some experiments, cells were preincubated with KN93 (1 μM), KN 92 (1 μM), chloroquine (40 μM), ammonium chloride (20 mM), MG132 (40 μM), and chlorpromazine (10 μM). For all of the experiments, cells were serum-starved overnight by incubation in media containing 0.5% (v/v) heat-inactivated FBS, then incubated in FBS-free media, with individual treatments noted in figure legends.

2.5. Lipolysis assay

Differentiated OP9 cells were treated as noted in the figure legends. Cells were incubated in media containing MEMα (without phenol red) and 1% fatty acid–free bovine serum albumin (BSA) (w/v). After 2 h of incubation, cells were treated with fresh MEMα (without phenol red) and 1% fatty acid–free BSA (w/v) media with or without 10 uM isoproterenol for 3–4 h. Insulin (100 nM) was added during the last 2–4 h of isoproterenol incubation as described in the figure legends. Media was collected and spun down at 2500 rpm for 5 min to pellet the detached cells. NEFA levels in the supernatant were measured using the NEFA enzymatic assay kit (Wako) according to manufacturer's instructions. The protein content of cell lysates was determined using the DC Protein Assay kit (BioRad), and secreted NEFA levels were normalized to protein content.

2.6. Protein extraction and immunoblotting

Adipose tissue samples and differentiated OP9 cells were homogenized in RIPA buffer (Thermo Fisher) supplemented with leupeptin, phenylmethylsulfonyl fluoride (PMSF), aprotinin, and okadaic acid (Sigma). Lysates were cleared by centrifugation at 15,000 rpm for 60 or 20 min at 4 °C for cells and tissue samples, respectively. Plasma membrane proteins were isolated as described previously [20]. Protein content of lysates was determined using the DC Protein Assay kit (BioRad). Protein extracts were electrophoresed on SDS-PAGE gels and transferred to PVDF membranes. The membranes were blocked for 1 h at room temperature in tris-buffered saline with 0.1% Tween 20

(TBST) containing 5% (w/v) BSA or nonfat milk. The membranes were then incubated at 4 °C overnight with primary antibodies in TBST containing 5% nonfat milk or BSA, followed by incubation with the appropriate secondary antibodies coupled to horseradish peroxidase. Proteins were detected by ECL chemiluminescence (Pierce). ImageJ was used for densitometric analysis of the immunoblots.

2.7. Quantitative RT-PCR analysis

Total RNA was extracted using TRIzol reagent (Invitrogen). cDNA was synthesized from 1 μg total RNA using oligo (dT) and Superscript II (Invitrogen). Quantitative RT-PCR was performed using the ABI Real Time PCR System and SYBR Green reagents (Applied Biosystems). To normalize the relative expression, a standard curve was prepared for each gene, with the expression level of each gene normalized to the 36B4 or HPRT gene (housekeeping).

2.8. Liver triglyceride analysis

Liver tissue was homogenized in PBS, and the lipids were isolated by the Folch extraction method (final chloroform/methanol/water solution = 8:4:3) [21]. The organic layer was collected and dried under nitrogen. The dried lipids were then reconstituted in 15% Triton X-100 in chloroform, which was evaporated with nitrogen and resuspended in water. TG concentrations were measured enzymatically (Wako Chemicals). To visualize lipid accumulation in hepatocytes, Hematoxylin & Eosin staining was performed on formalin-fixed liver sections.

2.9. Statistics

All results are presented as mean ± SEM. Statistical significance was determined using SigmaPlot software. Data that passed the normality test were analyzed using Student's t-test and ANOVA. Data that were not normally distributed were analyzed using the nonparametric Mann–Whitney U test. Significant differences were determined by repeated measures ANOVA for ITT and GTT. Differences were considered statistically significant at $p < 0.05$.

3. RESULTS

3.1. CAMK2γ and CAMK2δ are expressed in WAT and activated in fasting and obesity

CAMK2 has four different isoforms: α, β, γ, and δ, each of which is encoded by separate genes [22,23]. We first investigated which CAMK2 isoforms are expressed in adipose tissue and found that epididymal WAT (eWAT), inguinal WAT (iWAT), and BAT express γ and δ isoforms (Figure 1A). Previously, we showed that hepatic CAMK2 is activated during fasting and contributes to glucose homeostasis by regulating hepatic glucose production. Similarly, we found that CAMK2 phosphorylation, which is a measure of its activation state, was significantly increased upon fasting in eWAT, without any change in total CAMK2 levels (Figure 1B). As obesity and insulin resistance are characterized by alterations in cytosolic calcium and CAMK2 activation [5,24], we asked next whether CAMK2 activity is increased in obese adipose tissue. We observed that the level of phospho-T287-CAMK2, but not total CAMK2, was significantly higher in eWAT and BAT from diet-induced obese (DIO) mice compared to controls (Figure 1C). Similarly, the level of phospho-T287-CAMK2 was markedly higher in iWAT, eWAT, and BAT of *ob/ob* mice compared to WT mice. Thus adipose tissue CAMK2 is activated in fasting and obesity, which led us to explore the possibility that adipocyte CAMK2 may contribute to metabolic regulation in obesity.

3.2. Deletion of adipocyte CAMK2 improves glucose homeostasis in obese mice

To investigate the functional importance of CAMK2 in adult mice adipose tissue without interfering with embryonic or neonatal development, we established a mouse model, designated as Ai-CAMK2 KO mice, in which both *Camk2g* and *Camk2d* were deleted in adipocytes in an inducible manner. This was performed by crossing *Camk2d*$^{loxP/loxP}$ and *Camk2g*$^{loxP/loxP}$ mice with mice carrying a tamoxifen-inducible Cre ER^{T2} transgene under the control of adiponectin promoter (AdipoqCreER^{T2}) [15,16,25]. Littermate mice carrying floxed alleles but not the Cre ER^{T2}-transgene were used as controls. In two separate cohorts, we injected Ai-CAMK2 KO and control mice with tamoxifen for 5 consecutive days after 7 or 20 weeks of HFD feeding, then continued HFD feeding for a total period of 15 or 30 weeks, respectively. As expected, *Camk2g* and *Camk2d* mRNAs were lowered in different adipose tissue depots 8–10 weeks after tamoxifen treatment (Figure 2A and F). Consistent with previous reports [26], both DIO control and Ai-CAMK2 KO mice experienced initial weight loss following tamoxifen treatment. However, there were no differences in body weight between the groups throughout the study, and neither group displayed any developmental or behavioral defects (Figure S1). Moreover, food intake (2.73 ± 0.01 g versus 3.17 ± 0.28 g per mouse per day), plasma total cholesterol (143.18 ± 9.01 mg/dl versus 140.79 ± 13.85 mg/dl), and plasma triglyceride levels (55.00 ± 5.40 mg/dl versus 59.39 ± 5.57 mg/dl) were similar between the two groups. However, compared with control DIO mice, Ai-CAMK2 KO mice had lower plasma insulin levels and insulin resistance as measured by HOMA-IR (Figure 2B,C and G). Further, DIO Ai-CAMK2 KO mice exhibited significantly lower blood glucose levels during the glucose tolerance test and insulin tolerance test, suggesting an improvement in glucose tolerance (Figure 2D, E, H and I). Similar results were obtained in the 16-week HFD-fed control (*Camk2d*$^{loxP/loxP}$, *Camk2g*$^{loxP/loxP}$) and *Camk2d*$^{loxP/loxP}$, *Camk2g*$^{loxP/loxP}$, and Adipoq-Cre BAC–transgenic mice (A-CAMK2 KO), which express Cre in a non-inducible manner [27] (Figure S2). Of note, there were no differences in body weights between the two groups. These data indicate that CAMK2 inhibition in obese mice improves glucose metabolism.

3.3. Adipocyte CAMK2 regulates insulin-induced AKT activation

Insulin-stimulated phosphorylation of AKT (also known as protein kinase B, PKB) increases the translocation of glucose transporter GLUT4, which stimulates glucose uptake into adipose tissue. We therefore assessed the effect of CAMK2 deficiency on adipocyte insulin signaling by measuring adipose tissue S473-AKT phosphorylation in DIO mice injected with insulin through the portal vein. Consistent with improved glucose tolerance and enhanced insulin sensitivity, DIO Ai-CAMK2 KO mice displayed significant increases in insulin-mediated AKT activation in both eWAT and iWAT (Figure 3A and B). To gain further mechanistic insight, we moved to an *in vitro* adipocyte model using bone marrow–derived stromal cell (OP9) differentiated adipocytes, which is a known *in vitro* model for the study of adipocyte metabolism [28–30]. Consistent with the *in vivo* findings, we observed that silencing *Camk2* improved insulin-stimulated S473-AKT phosphorylation in cultured adipocytes, which suggests that the effect of CAMK2 deficiency on insulin signaling is cell-intrinsic (Figure 3C). We next investigated the

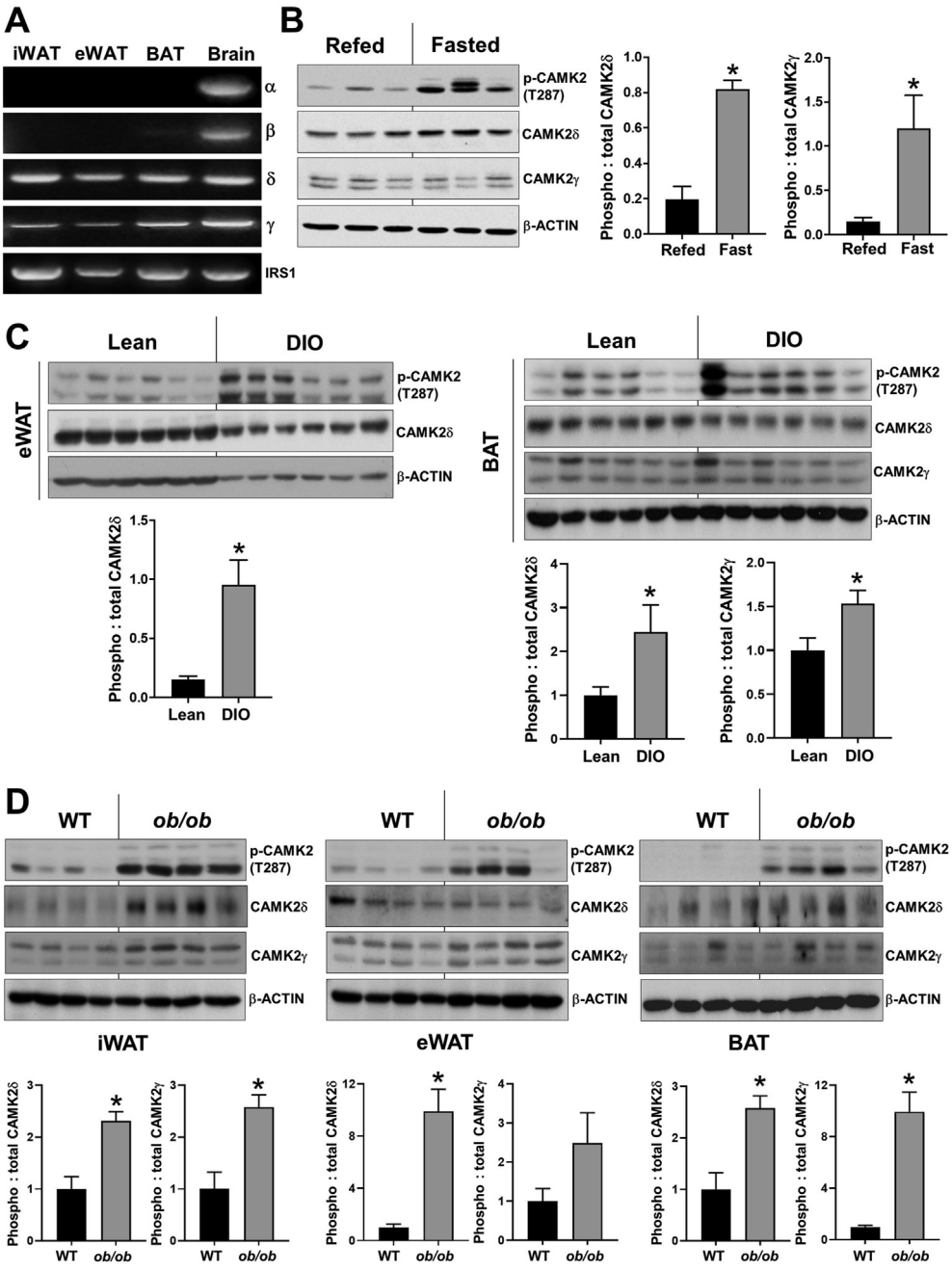

Figure 1: CAMK2 is expressed in adipose tissue and activated in fasting and obesity. (**A**) RNA from iWAT, eWAT, BAT, and brain tissue of a WT mouse were probed for the indicated *Camk2* isoform mRNAs or *Irs1* (internal control) by RT-PCR. (**B**) WT mice were fasted for 12 h (fasted) and then refed for 1 h (refed). Total protein extracts of eWAT were then assayed for phospho-T287-CAMK2, CAMK2γ, CAMK2δ, and β-ACTIN by immunoblot. Densitometric quantification of data is shown in the bar graphs (n = 3 mice per group). (**C**) phospho-T287-CAMK2, CAMK2δ, CAMK2γ, and β-ACTIN levels from eWAT and BAT of lean (control) and DIO mice were analyzed. Densitometric quantification of data is shown in the bar graphs (n = 6 mice per group). (**D**) iWAT, eWAT, and BAT extracts from 10-week-old WT and *ob/ob* mice were probed for phospho-T287-CAMK2, CAMK2δ, CAMK2γ, and β-ACTIN by immunoblot. Densitometric quantification of data is shown in the bar graphs (n = 4 mice per group).

response of control and CAMK2-deficient adipocytes to saturated fatty acid palmitate treatment, which has been shown to attenuate insulin signaling [31–33]. We found that the decrease in insulin-stimulated phospho-S473-AKT levels upon palmitate treatment was completely abrogated by silencing adipocyte *Camk2* (Figure 3D). To further establish a role for CAMK2 in adipocyte insulin signaling, we transduced adipocytes with an adenovirus encoding a constitutively-active, mutant form of CAMK2 (T287D, CA-CAMK2), which results in autonomous activity [19]. We observed that CA-CAMK2 treatment was sufficient to interfere with insulin action, as exemplified by the inhibition of insulin-induced phospho-S473-AKT (Figure 3E).

3.4. CAMK2 regulates adipocyte insulin signaling through its effects on INSR levels

Our previous work in hepatocytes revealed that CAMK2 inhibition enhances activation of AKT via suppressing pseudokinase tribbles 3

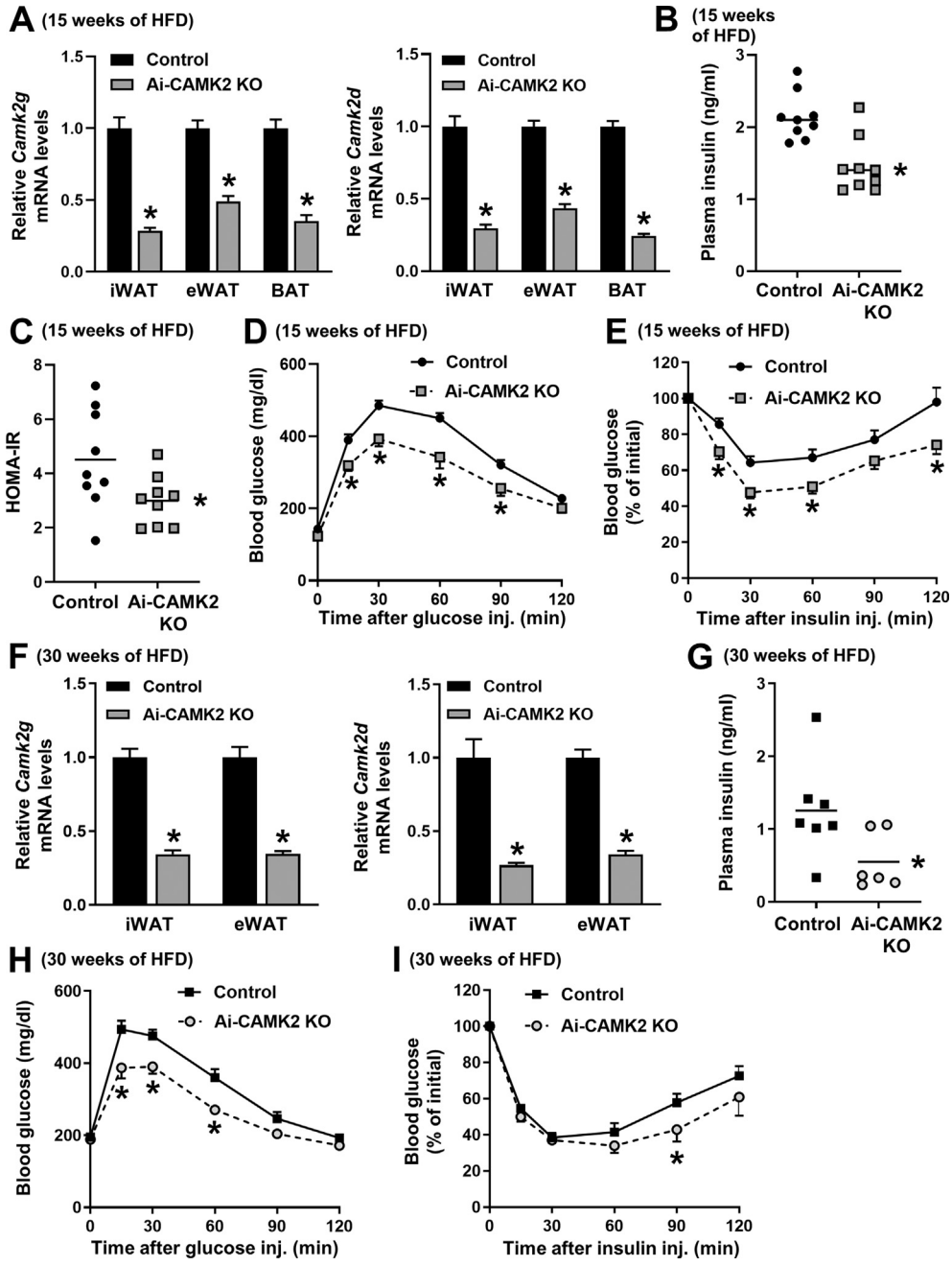

Figure 2: Deletion of adipocyte CAMK2 improves glucose homeostasis in obese mice. Two separate cohorts of Ai-CAMK2 KO and control mice that were fed with HFD for a total of 15 and 30 weeks were i.p. injected with tamoxifen. (**A**) mRNA levels of *Camk2g* and *Camk2d* in eWAT, iWAT, and BAT, (**B**) plasma insulin levels, (**C**) HOMA-IR, (**D**) glucose tolerance test, and (**E**) insulin tolerance test in Ai-CAMK2 KO and control mice that were treated with tamoxifen after being fed with HFD for 15 weeks ($n = 9$ mice per group; mean $\pm$ SEM, $p < 0.05$). (**F**) mRNA levels of *Camk2g* and *Camk2d* in eWAT and iWAT, (**G**) plasma insulin levels, (**H**) glucose tolerance test, and (**I**) insulin tolerance test in control and Ai-CAMK2 KO mice that were treated with tamoxifen after being fed with HFD for 30 weeks ($n = 6–7$ mice per group; mean $\pm$ SEM, $p < 0.05$).

(TRB3), which is an inhibitor of insulin-induced phosphorylation of AKT [9,34]. We therefore asked whether adipocyte CAMK2 deficiency increases insulin-AKT signaling by regulating TRB3 levels. Remarkably, we did not observe any changes in *Trb3* mRNA levels in control versus Ai-CAMK2 KO eWAT or CAMK2-deficient adipocytes, suggesting that TRB3 does not participate in the CAMK2-mediated regulation of insulin signaling in adipose tissue (Figure S3A and B). Next, we focused our attention on the activation of proximal insulin signaling component INSR, which is downregulated in adipose tissues of both obese animal and human subjects [35–37]. We observed that silencing *Camk2* in cultured adipocytes significantly improved INSR activity, as shown by increased Y1150/1151 phosphorylation of INSR compared to scramble-treated controls (Figure 4A). Interestingly, INSR protein analysis revealed that CAMK2 deficiency enhanced INSR activity by increasing the levels of total INSR, which led to more functional and cell surface–localized INSR (Figure 4A and B). To confirm these findings, we used the CAMK2 inhibitor KN93 and showed that this compound, but not the

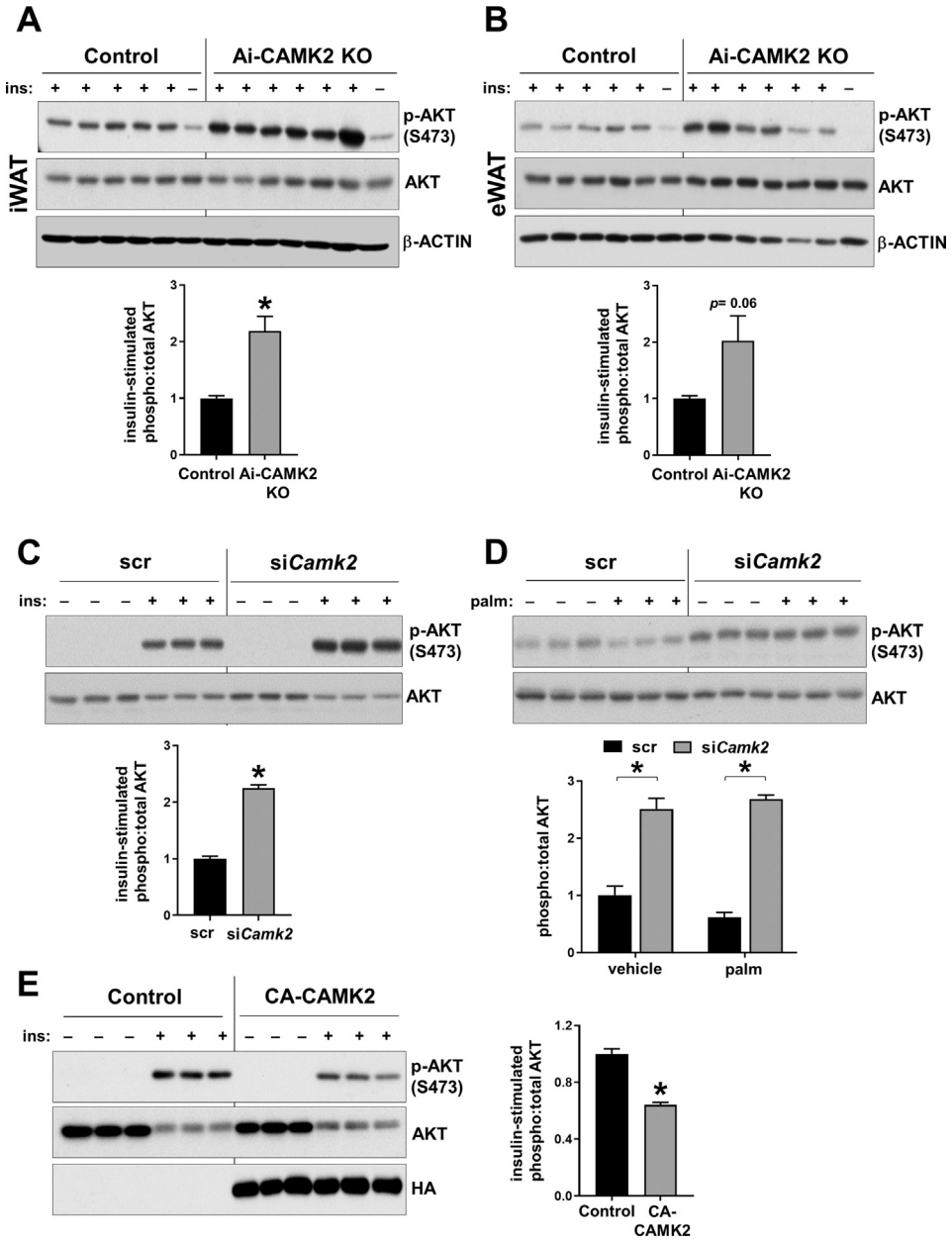

Figure 3: Adipocyte CAMK2 regulates insulin-induced AKT activation. (**A**—**B**) Ai-CAMK2 KO and control mice that were fed with HFD for 30 weeks were injected with 0.6 IU/kg insulin (ins) through the portal vein after 5 h of fasting. iWAT (A) and eWAT (B) extracts were then assayed for phospho-S473-AKT, total AKT, and β-ACTIN by immunoblot. Densitometric quantification is shown in the bar graph (n = 6—7 mice per group). (**C**) Insulin (ins)-stimulated phospho-S473-AKT and total AKT levels were assayed in differentiated OP9 cells treated with control siRNA (scr) or siRNAs against *Camk2g* and *Camk2d* (si*Camk2*). Densitometric quantification is shown in the bar graph (n = 3 technical replicates per group). (**D**) Similar to C, except that the cells were treated with or without 100 μM palmitate (palm) for 6 h followed by 5 min of insulin (ins) stimulation. Densitometric quantification is shown in the bar graph (n = 3 technical replicates per group). (**E**) Similar to C, except that the cells were treated with control adenovirus (LacZ) or an adenovirus expressing the CA-CAMK2 that has an HA tag. Densitometric quantification is shown in the bar graph (n = 3 technical replicates per group).

structurally related inactive homologue KN92, significantly increased INSR protein levels (Figure 4C). Conversely, transduction of adipocytes with CA-CAMK2 decreased INSR levels and activity compared to control virus expressing LacZ (Figure 4D). As obesity-associated chronic hyperinsulinemia has been shown to downregulate INSR in many cells, including adipocytes, we next investigated whether CAMK2 deficiency protects against INSR downregulation upon chronic exposure to high concentrations of insulin. We found that the decrease in INSR levels upon chronic insulin treatment was abrogated by silencing adipocyte CAMK2 (Figure 4E). Then, we returned to our *in vivo* model by analyzing INSR in DIO Ai-CAMK2 KO versus obese control mice and observed significantly higher INSR levels in eWAT and iWAT of DIO Ai-CAMK2 KO (Figure 4F). In order to determine the molecular mechanism(s) of adipocyte INSR regulation by CAMK2, we analyzed *Insr* mRNA levels in CAMK2-deficient adipose tissue and cultured adipocytes and observed no significant changes (Figure S3C—F). Similarly, CA-CAMK2 treatment had no effect on *Insr* mRNA in differentiated adipocytes (Figure S3G). Altogether, these results suggest that CAMK2 regulates insulin signaling by controlling INSR protein but not *Insr* mRNA.

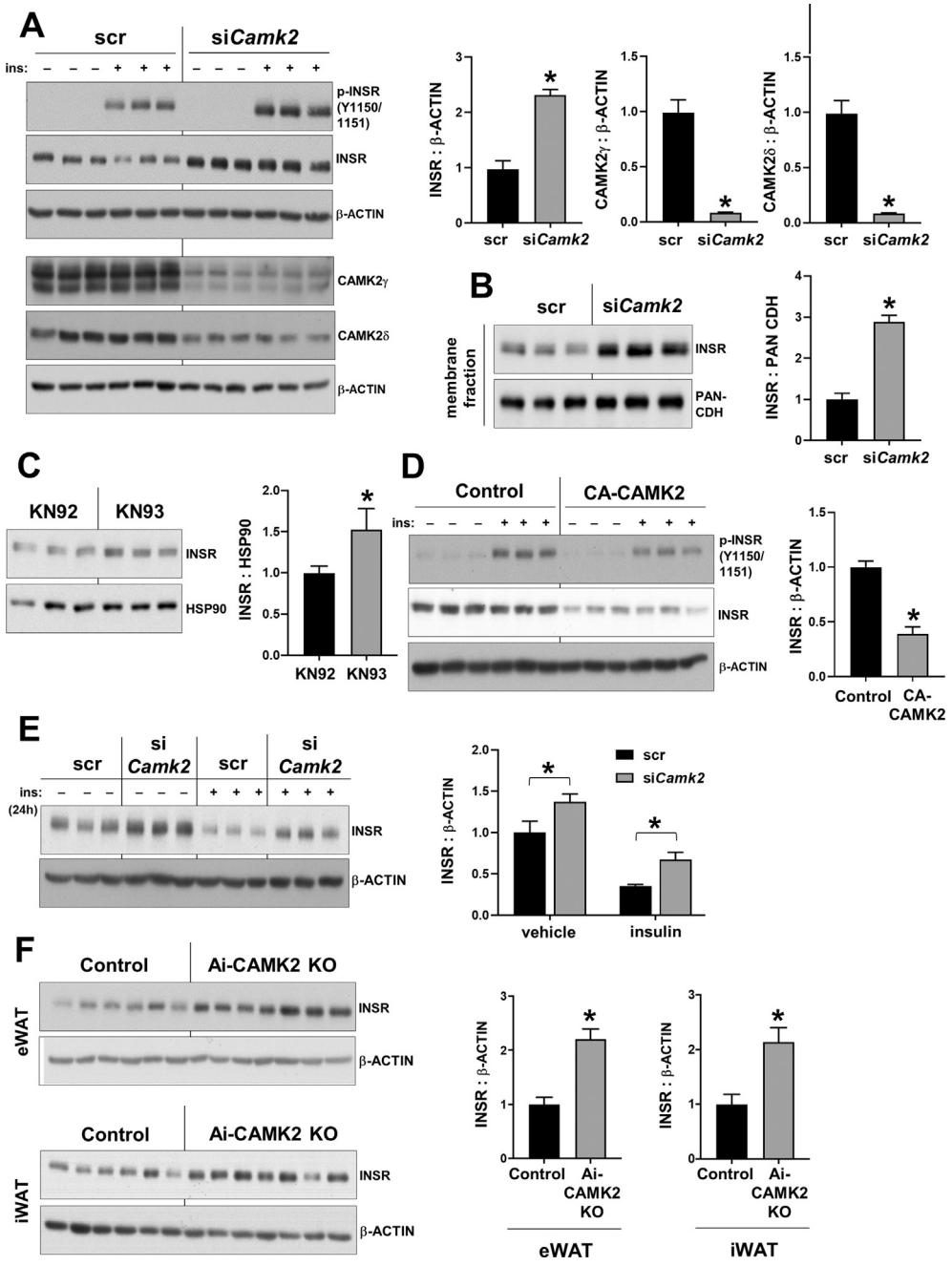

Figure 4: CAMK2 regulates adipocyte INSR levels. (**A**) Insulin-stimulated phospho-Y1150/1151-INSR, total INSR, CAMK2γ, CAMK2δ, and β-ACTIN levels were assayed in differentiated OP9 cells treated with control siRNA (scr) or siRNAs against *Camk2g* and *Camk2d* (si*Camk2*). Densitometric quantification of data is shown in the bar graphs (n = 3 technical replicates per group). (**B**) Plasma membrane protein extracts from OP9 cells treated with control siRNA (scr) or siRNAs against *Camk2g* and *Camk2d* (si*Camk2*) were probed for INSR and loading control, PAN-CDH (pan cadherin) by immunoblot. Densitometric quantification is shown in the bar graph (n = 3 technical replicates per group). (**C**) Total INSR and HSP90 levels were assayed in differentiated OP9 cells treated with 1 μm of either KN93 or its inactive homolog KN92. Densitometric quantification is shown in the bar graph (n = 3 technical replicates per group). (**D**) Similar to A, except that the cells were treated with control adenovirus (LacZ) or an adenovirus expressing the CA-CAMK2. Densitometric quantification is shown in the bar graph (n = 3 technical replicates per group). (**E**) Differentiated OP9 cells were treated with control siRNA (scr) or siRNAs against *Camk2g* and *Camk2d* (si*Camk2*). The cells were then incubated with insulin (ins) for 24 h, and total INSR levels were analyzed. Densitometric quantification is shown in the bar graph (n = 3 technical replicates per group). (**F**) Total INSR levels were assayed in eWAT and iWAT of DIO Ai-CAMK2 KO or control obese mice that were fed with HFD for 30 weeks. Densitometric quantification of data is shown in the bar graphs (n = 6–7 mice per group).

3.5. CAMK2 activation lowers INSR via clathrin-mediated lysosomal degradation

INSR is a receptor tyrosine kinase (RTK), and upon insulin binding, it is endocytosed via either clathrin-coated vesicles or caveolae [38]. In normal physiology, a majority of the endocytosed INSR is recycled back to the plasma membrane, with a small portion routed to lysosomes for degradation [39]. In this regard, prevention of RTK internalization and degradation has been hypothesized to result in

constitutive activation and prolonged signaling [40]. As CAMK2 did not affect the mRNA levels of *Insr*, we tested whether CAMK2 regulates the endocytosis of INSR. We first showed that treatment of adipocytes with the caveolin-mediated endocytosis inhibitor, filipin, was not able to prevent the CA-CAMK2—induced INSR decrease, suggesting that CAMK2 does not affect caveolin-regulated INSR endocytosis (Figure 5A). Next, we inhibited clathrin-mediated endocytosis by treating the cells with 10 μM chlorpromazine and found that this treatment abrogated the decrease in INSR conferred by CA-CAMK2 overexpression (Figure 5B). Of note, level of transferrin receptor (TFRC1), which is internalized through clathrin-mediated endocytosis, was not increased in CAMK2-deficient adipocytes or in eWAT and iWAT of DIO Ai-CAMK2 KO, suggesting that CAMK2 specifically regulates the clathrin-mediated internalization of INSR without affecting TFRC1 (Figure 5C and D). As endocytosed INSR is degraded in proteasomes and lysosomes [38,41], we next checked whether INSR degradation is regulated by CAMK2. We found that treatment of cells with the proteasome inhibitor, MG132 (40 μM), had no effect on CA-CAMK2—mediated decrease in INSR, whereas disruption of lysosomal function via chloroquine (40 μM) or ammonium chloride (20 mM) treatment prevented the CA-CAMK2—induced INSR decrease (Figure 5E—G). Collectively, these data show that adipocyte CAMK2 regulates insulin signaling via its effects on clathrin-mediated endocytosis and lysosomal degradation of INSR.

3.6. CAMK2 contributes to the regulation of adipocyte lipolysis

Adipose tissue insulin signaling regulates plasma free fatty acid (FFA) levels via suppressing lipolysis, and high circulating FFAs contribute to obesity-induced metabolic dysfunction [42]. Given that adipocyte-CAMK2 deficiency enhances insulin signaling, we analyzed plasma NEFA and glycerol levels in DIO Ai-CAMK2 KO versus control obese mice. Consistent with improved adipocyte insulin signaling, we found

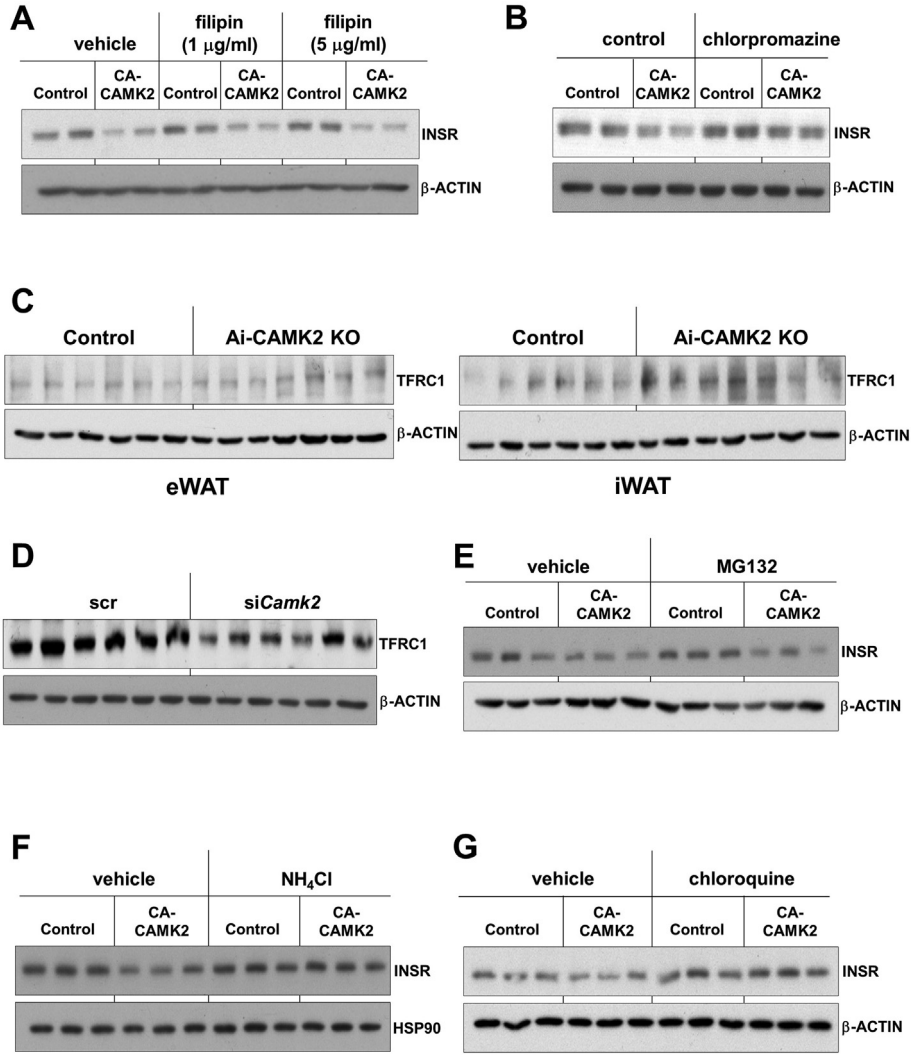

Figure 5: CAMK2 activation lowers INSR via clathrin-mediated lysosomal degradation. (**A**) Differentiated OP9 cells treated with control adenovirus (LacZ) or CA-CAMK2 were incubated with indicated amounts of filipin for 6 h. Total protein extracts were assayed for INSR and β-ACTIN by immunoblot (n = 2 technical replicates per group). (**B**) Similar to A, except that the cells were incubated with 10 μM chlorpromazine (n = 2 technical replicates per group). (**C**—**D**) Transferrin receptor 1 (TFRC1) and β-ACTIN levels were assayed in eWAT and iWAT of obese Ai-CAMK2 KO and control mice (C), and adipocytes treated with control siRNA (scr) or siRNAs against *Camk2g* and *Camk2d* (si*Camk2*) (D) (n = 6—7 mice per group and n = 6 technical replicates per group, respectively). (**E**—**G**) Differentiated OP9 cells treated with control adenovirus (LacZ) or CA-CAMK2 were incubated with 40 μM MG132 (E), 20 mM ammonium chloride (NH_4Cl) (F), or 40 μM chloroquine (G) for 6 h, and INSR, β-ACTIN, or HSP90 levels were assayed by immunoblot (n = 3 technical replicates per group).

that DIO Ai-CAMK2 KO mice had lower circulating NEFA and glycerol under both fasting and refeeding conditions (Figure 6A and B). As suppression of lipolysis decreases ketogenic substrate flux to the liver, we next assessed circulating β-hydroxybutyrate levels. While fasting Ai-CAMK2 KO mice trended only towards lower β-hydroxybutyrate levels, suppression of β-hydroxybutyrate following a 2-hr refeeding period in Ai-CAMK2 KO mice was significantly lower (Figure 6C). Moreover, we found that Ai-CAMK2 KO mice liver had fewer lipid droplets and decreased triglyceride content, indicating that Ai-CAMK2 KO mice are protected from obesity-induced fatty liver formation (Figure 6D). In line with an improvement in hepatic steatosis, insulin-stimulated phospho-S473-AKT levels in the livers of Ai-CAMK2 KO mice were significantly increased (Figure S3H). This supports the idea that adipocyte-CAMK2 deficiency results in enhanced hepatic insulin sensitivity, which is consistent with an improvement in systemic glucose metabolism. As with the *in vivo*

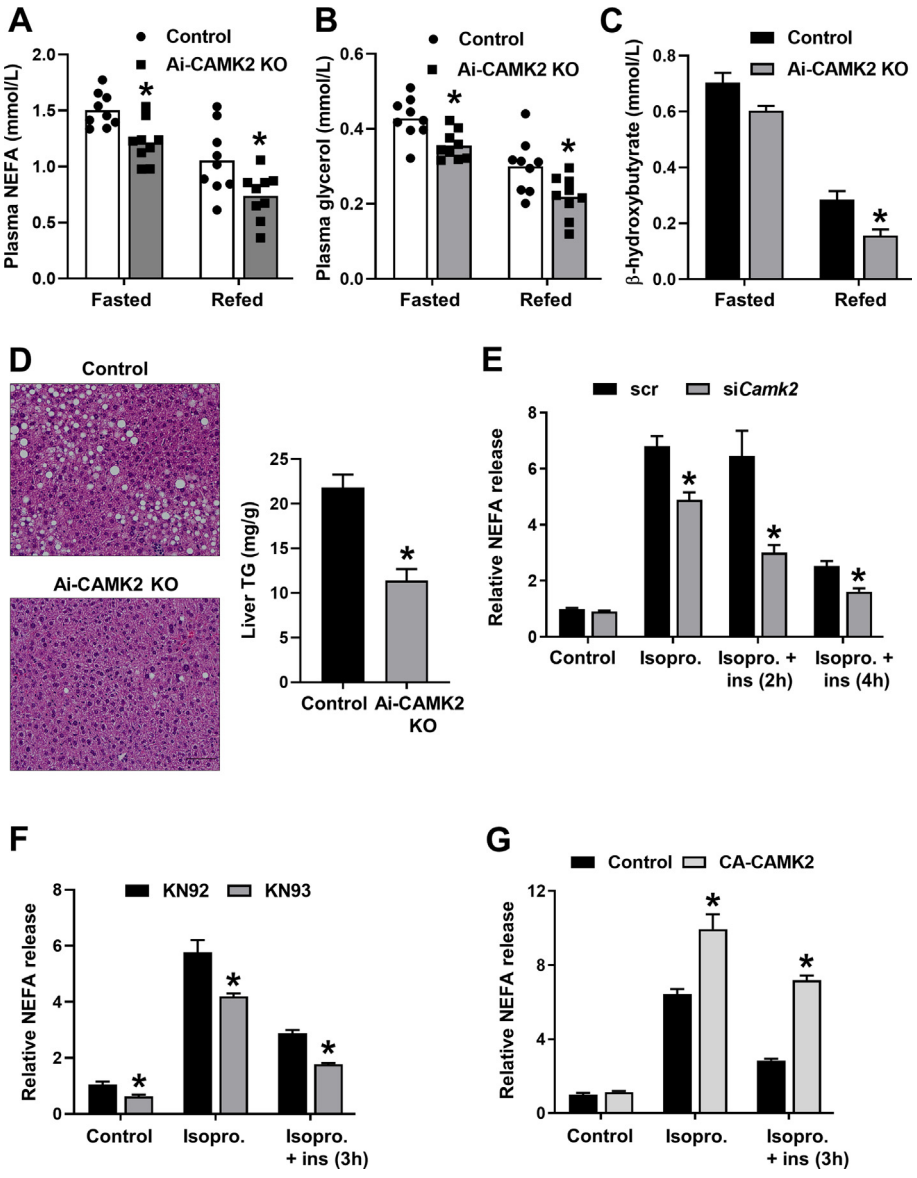

Figure 6: CAMK2 regulates adipocyte lipolysis (**A**–**B**) Plasma NEFA and glycerol levels were measured from overnight-fasted (fasted) and overnight-fasted and then refed (refed) DIO Ai-CAMK2 KO or control obese mice that were fed with HFD for 15 weeks (n = 9 mice per group; mean ± SEM, $p < 0.05$). (**C**) Plasma β-hydroxybutyrate levels were measured from overnight-fasted (fasted), and overnight-fasted and then refed (refed) DIO Ai-CAMK2 KO or control obese mice that were fed with HFD for 15 weeks (n = 4–5 mice per group; mean ± SEM, $p < 0.05$). (**D**) Representative images of H&E staining of liver sections in DIO Ai-CAMK2 KO or control obese mice. Scale bar, 50 μm. Liver triglyceride (TG) content is measured in DIO Ai-CAMK2 KO or control obese mice that were fed with HFD for 15 weeks (n = 4 mice per group; mean ± SEM, $p < 0.05$). (**E**) Control siRNA (scr) or siRNAs against *Camk2g*- and *Camk2d* (si*Camk2*)-treated adipocytes were incubated with isoproterenol (isopro.) for 3 h. The cells were then treated with 100 nM insulin (ins) or vehicle control for an additional 2 or 4 h in the presence of isoproterenol, and secreted NEFA levels were analyzed. The data are normalized to intracellular protein concentration and presented as relative to control (n = 3 technical replicates per group). (**F**) Adipocytes that were pretreated with 1 μM of either KN93 or its inactive homolog KN92 for 1 h were incubated with isoproterenol (isopro.) for 3 h. The cells were then treated with 100 nM insulin (ins) or vehicle control for 3 more hr in the presence of isoproterenol, and secreted NEFA levels were analyzed. The data are normalized to intracellular protein concentration and presented as relative to control (n = 3 technical replicates per group). (**G**) Similar to E, except that the cells were treated with control adenovirus (LacZ) or an adenovirus expressing the CA-CAMK2, and the insulin treatment was for 3 h. The data are normalized to intracellular protein concentration and presented as relative to control (n = 3 technical replicates per group).

data, we observed that CAMK2-deficient or KN93-treated adipocytes released significantly less FFA upon the β-adrenergic stimulator isoproterenol, and addition of insulin further suppressed this response (Figure 6E and F). In contrast, CA-CAMK2—treated cells had high isoproterenol-stimulated FFA release and responded poorly to insulin's suppressive effect on lipolysis (Figure 6G). These combined data support the hypothesis that adipocyte-CAMK2 contributes to the regulation of lipolysis.

3.7. Adipocyte CAMK2 regulates TNFα-induced inflammation and insulin resistance

Lipolysis stimulates macrophage infiltration in eWAT [3,43], and inflamed adipocytes further contribute to the inflammatory milieu by secreting proinflammatory mediators. Therefore, we next sought to determine whether there was a link between CAMK2 and adipocyte immune response. In this regard, previous work in cardiomyocytes and macrophages have suggested a role for activated CAMK2 in propagating the inflammatory process [44,45]. Similarly, we observed that CAMK2-deficient adipocytes had markedly lower levels of mRNAs encoding proinflammatory mediators, including *Cxcl10*, *Ccl1*, *Ccl5*, *Fas,* and *Saa3,* upon TNFα stimulation (Figure 7A). As proinflammatory cytokines activate c-Jun N-terminal kinase (JNK) and block insulin signaling, we next checked phospho-T183/Y185-JNK as a measure of JNK activity. The data showed that CAMK2-deficient adipocytes had lower JNK phosphorylation upon TNFα and palmitate treatment (Figure 7B and C), as previously shown in other cell types [46,47].

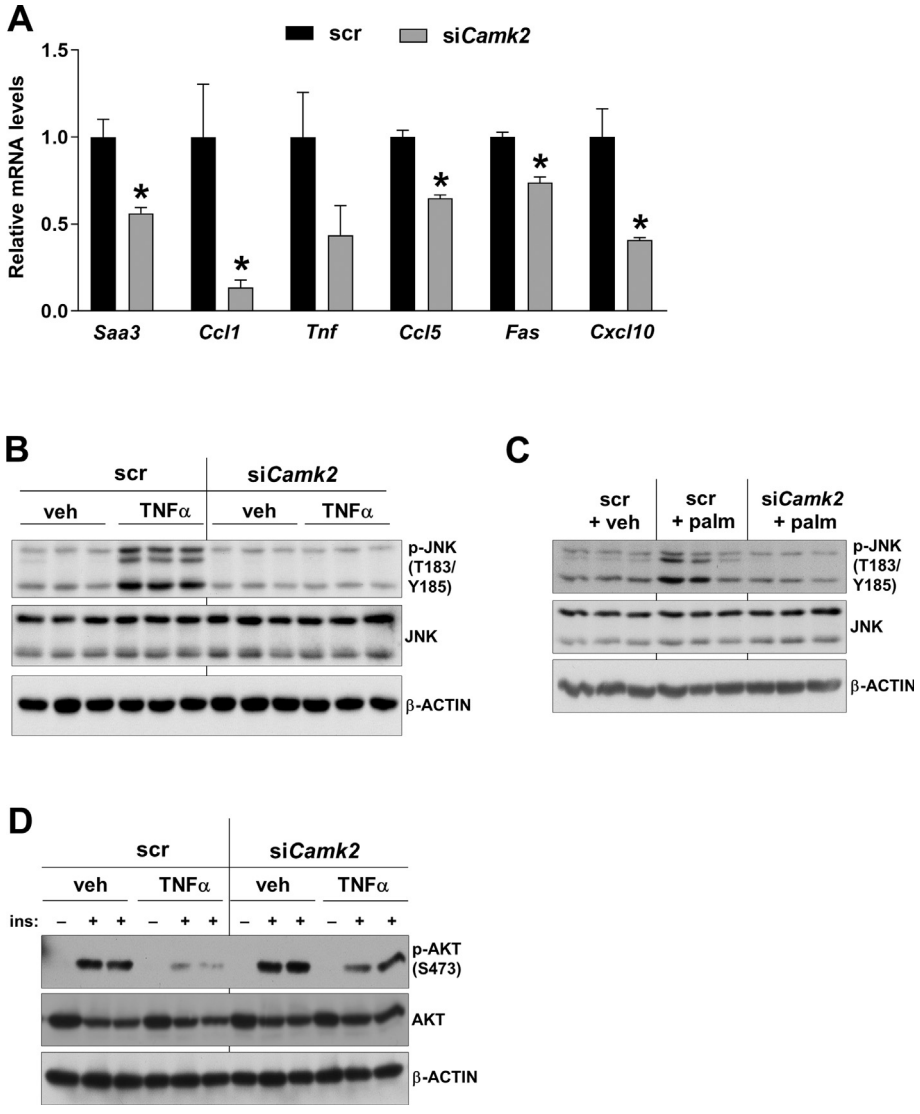

Figure 7: CAMK2 contributes to TNFα-induced inflammation and insulin resistance. (**A**) Control siRNA (scr) or siRNAs against *Camk2g*- and *Camk2d* (si*Camk2*)-treated adipocytes were incubated with 50 ng/mL TNFα for 14 h, and *Saa3*, *Ccl1*, *Tnf*, *Ccl5*, *Fas,* and *Cxcl10* mRNA levels were analyzed (n = 3 technical replicates per group). (**B**) Similar to A, except that the cells were treated with TNFα for 6 h and phospho-T183/Y185-JNK, total JNK, and β-ACTIN levels were analyzed (n = 3 technical replicates per group). (**C**) Control siRNA (scr) or siRNAs against *Camk2g*- and *Camk2d* (si*Camk2*)-treated adipocytes were incubated with 250 μM palmitate for 6 h, and phospho-T183/Y185-JNK, total JNK, and β-ACTIN levels were analyzed (n = 3 technical replicates per group). (**D**) Similar to A, except that the cells were treated with or without 100 nM insulin (ins) for 5 min after 14 h of TNFα or vehicle (veh) incubation, and lysates were probed for phospho-S473-AKT, total AKT, and β-ACTIN by immunoblot.

Finally, consistent with lower proinflammatory cytokines and JNK activation, we found that CAMK2 silencing abrogated the TNFα-induced inhibition of phospho-S473-AKT in adipocytes (Figure 7D). These results suggest that adipocyte CAMK2 regulates lipolysis and contributes to TNFα-induced inflammation and inhibition of insulin signaling, which may be additional underlying mechanisms contributing to metabolic regulation by CAMK2.

4. DISCUSSION

Recent work has demonstrated potential in targeting CAMK2 in the regulation of systemic metabolic control. Inhibition of hepatic CAMK2 improves liver insulin signaling, obesity-associated glucose intolerance, and insulin resistance [8,9]. Similarly, CAMK2 deficiency enhances skeletal muscle INSR signaling and glucose transport in diabetic mice [13]. Here, we expand upon these observations and provide evidence that inhibiting adipocyte CAMK2 also exerts beneficial effects in treating obesity-associated glucose intolerance. We show that adipocyte CAMK2 activity is increased in obesity, and deficiency of CAMK2 in adipose tissue increases INSR levels and inhibits adipocyte inflammation, which correlates with metabolic improvement. In agreement with the findings described here, genome-wide association studies (GWAS) have identified an SNP near the *CAMK2G* gene (rs2633310) that is relevant to T2D [48]. eQTL data extracted from the GTExPortal suggests that the common variant (rs2633310-T), which confers a lower T2D risk, associates with decreased expression of *CAMK2G* in human subcutaneous adipose tissue, suggesting a possible genetic link to human disease.

The underlying mechanisms leading to CAMK2 activation in obese adipose tissue are likely diverse. One of the major mechanisms by which CAMK2 becomes activated is -upon an increase in cytosolic calcium [49]. In this regard, recent work has shown that inflammation-induced JNK activation in WAT enhances the expression and activity of ITPR, which results in increased cytosolic calcium and CAMK2 activation [50]. As adipocyte CAMK2 also regulates JNK activation (Figure 7B and C), it is possible that the JNK-ITPR-CAMK2 pathway is part of a positive feedback amplification cycle responding to inflammatory and metabolic signals in obesity. Other mechanisms of CAMK2 activation, including oxidation and O-GlcNAc modification, may also contribute to increased CAMK2 activity [49]. Of note, both reactive oxygen species (ROS) accumulation and O-GlcNAc modification are increased in eWAT of obese and diabetic human subjects and mouse models, resulting in dysregulated adipocytokine secretion and impaired adipose tissue glucose transport [51–54]. As antioxidants improve glucose homeostasis in mouse models of insulin resistance and inhibit CAMK2 activity in other cell types, it is possible that one mechanism of this metabolic improvement could be related to antioxidant treatment–mediated CAMK2 inhibition [55,56]. Another important finding of our study is that the fasting signal–activated CAMK2 in WAT plays a role in the regulation of lipolysis. In this regard, we have previously shown that fasting increases hepatocyte CAMK2 activity via glucagon-mediated activation of protein kinase A (PKA), which phosphorylates and activates ITPR [8,57]. Although the WAT glucagon receptor mRNA transcript level is severalfold lower than that of liver [58], it is possible that a similar glucagon receptor–ITPR pathway in WAT contributes to CAMK2 activation upon fasting. Increased catecholamine release during fasting likely amplifies this process by activating PKA [59].

Intact insulin signaling is essential for the maintenance of normal adipose tissue mass and function. Defects in adipocyte insulin action result in systemic insulin resistance [60,61], whereas enhanced insulin signaling improves whole-body glucose homeostasis [62]. Reduced INSR level is an important underlying cause of adipose tissue insulin resistance. Mechanistically, clathrin- and caveolin-dependent endocytosis pathways have been reported to terminate INSR signaling and regulate INSR degradation [38]. Previous work has shown that CAMK2 promotes the $GABA_B$ receptor endocytosis in neurons [63]. Consistent with these findings, our results suggest a specific role for adipocyte CAMK2 in the regulation of clathrin-mediated INSR endocytosis and degradation. As clathrin-associated sorting proteins, adaptor protein 2 (AP2) complex and spindle checkpoint proteins are known to regulate clathrin-mediated INSR endocytosis, future studies will examine whether these proteins are targeted by CAMK2 [64].

The degree of macrophage infiltration of WAT correlates with insulin resistance in both mouse models and human studies [65–67]. Inflamed adipocytes further contribute to the inflammatory milieu by secreting proinflammatory mediators, including TNFα, which disrupt adipocyte metabolism [68]. Although the underlying molecular mechanisms that initiate and sustain WAT inflammation are complex, growing evidence indicates that high circulating plasma insulin and FFA levels as well as disrupted calcium homeostasis and insulin signaling are involved in this regulation [3,50,62,69]. Given that CAMK2 is causally linked to these processes, it is not surprising that CAMK2 occupies a proinflammatory role in adipocytes. Our results showing that CAMK2 silencing protects against inflammation and inflammation-associated insulin resistance (Figure 7) suggest that a suppressed inflammatory response via CAMK2 inhibition may also contribute to the observed insulin-sensitive phenotype in obese mice. Future work is needed to determine whether activation of CAMK2 correlates with WAT inflammation in humans.

Brown and beige adipocytes regulate thermogenesis and energy expenditure. In this regard, our data showing increased CAMK2 activity in both DIO and *ob/ob* BAT indicate that CAMK2 may play a role in obesity-induced BAT function. Brown and beige adipocytes express UCP1 and are responsive to insulin. Interestingly, mice with insulin receptor deficiency in UCP1-positive cells did not exhibit systemic insulin resistance compared to mice with insulin receptor deletion in both white and brown adipocytes [2]. While our data suggest that the improvement in WAT insulin signaling resulted in the overall glucose-sensitive phenotype of Ai-CAMK2 KO mice, it is possible that CAMK2's effects in BAT function could have also contributed to the observed improved metabolism. Although we did not detect gross changes in BAT morphology in Ai-CAMK2 KO mice, the role of CAMK2 in brown/beige adipocytes and thermogenesis could be an important topic for future investigation.

5. CONCLUSIONS

In summary, our results show that adipocyte CAMK2 regulates obesity-induced glucose homeostasis. Deficiency or inhibition of adipocyte CAMK2 improves insulin signaling and obesity-associated glucose intolerance. CAMK2 also contributes to the regulation of adipocyte lipolysis and inflammation. Thus adipocyte-specific CAMK2 inhibition could be beneficial against metabolic dysfunction.

AUTHORS' CONTRIBUTIONS

W.D. designed and performed the experiments, analyzed the data, interpreted results, and wrote the manuscript. M.C. and S.P. designed and performed the experiments, analyzed the data, and interpreted results. H.A.S. provided critical reagents and advice related to CAMK2. L.O. conceived and supervised the project, designed experiments,

analyzed data, interpreted results, and wrote and revised the manuscript.

ACKNOWLEDGMENTS

The authors would like to thank Dr. Eric N. Olson and his lab (UT Southwestern) for providing the *Camk2g*$^{fl/fl}$ and *Camk2d*$^{fl/fl}$ mice. This work was supported by NIH grants DK106045 and DK124457 to L.O., HL049426 to H.A.S., and a State Scholarship Fund from China Scholarship Council (201806370080) to W.D.

CONFLICT OF INTEREST

The authors declare no competing interests.

APPENDIX A. SUPPLEMENTARY DATA

Supplementary data to this article can be found online at https://doi.org/10.1016/j.molmet.2021.101300.

REFERENCES

[1] Scherer, P.E., 2019. The many secret lives of adipocytes: implications for diabetes. Diabetologia 62(2):223–232.

[2] Czech, M.P., 2020. Mechanisms of insulin resistance related to white, beige, and brown adipocytes. Molecular Metabolism 34:27–42.

[3] Kosteli, A., Sugaru, E., Haemmerle, G., Martin, J.F., Lei, J., Zechner, R., et al., 2010. Weight loss and lipolysis promote a dynamic immune response in murine adipose tissue. Journal of Clinical Investigation 120(10):3466–3479.

[4] Xu, X., Grijalva, A., Skowronski, A., van Eijk, M., Serlie, M.J., Ferrante Jr., A.W., 2013. Obesity activates a program of lysosomal-dependent lipid metabolism in adipose tissue macrophages independently of classic activation. Cell Metabolism 18(6):816–830.

[5] Segal, S., Lloyd, S., Sherman, N., Sussman, K., Draznin, B., 1990. Postprandial changes in cytosolic free calcium and glucose uptake in adipocytes in obesity and non-insulin-dependent diabetes mellitus. Hormone Research 34(1):39–44.

[6] Baumbach, J., Hummel, P., Bickmeyer, I., Kowalczyk, K.M., Frank, M., Knorr, K., et al., 2014. A Drosophila in vivo screen identifies store-operated calcium entry as a key regulator of adiposity. Cell Metabolism 19(2):331–343.

[7] Subramanian, M., Metya, S.K., Sadaf, S., Kumar, S., Schwudke, D., Hasan, G., 2013. Altered lipid homeostasis in Drosophila InsP3 receptor mutants leads to obesity and hyperphagia. Disease Models & Mechanisms 6(3):734–744.

[8] Ozcan, L., Wong, C.C., Li, G., Xu, T., Pajvani, U., Park, S.K., et al., 2012. Calcium signaling through CaMKII regulates hepatic glucose production in fasting and obesity. Cell Metabolism 15(5):739–751.

[9] Ozcan, L., Cristina de Souza, J., Harari, A.A., Backs, J., Olson, E.N., Tabas, I., 2013. Activation of calcium/calmodulin-dependent protein kinase II in obesity mediates suppression of hepatic insulin signaling. Cell Metabolism 18(6):803–815.

[10] Ozcan, L., Ghorpade, D.S., Zheng, Z., de Souza, J.C., Chen, K., Bessler, M., et al., 2016. Hepatocyte DACH1 is increased in obesity via nuclear exclusion of HDAC4 and promotes hepatic insulin resistance. Cell Reports 15(10):2214–2225.

[11] Wang, Y., Yan, S., Xiao, B., Zuo, S., Zhang, Q., Chen, G., et al., 2018. Prostaglandin F2alpha facilitates hepatic glucose production through CaMKII-gamma/p38/FOXO1 signaling pathway in fasting and obesity. Diabetes 67(9):1748–1760.

[12] Perry, R.J., Zhang, D., Guerra, M.T., Brill, A.L., Goedeke, L., Nasiri, A.R., et al., 2020. Glucagon stimulates gluconeogenesis by INSP3R1-mediated hepatic lipolysis. Nature 579(7798):279–283.

[13] Chen, J., Fleming, T., Katz, S., Dewenter, M., Hofmann, K., Saadatmand, A., et al., 2021. CaM kinase II-delta is required for diabetic hyperglycemia and retinopathy but not nephropathy. Diabetes 70(2):616–626.

[14] Ozcan, L., Xu, X., Deng, S.X., Ghorpade, D.S., Thomas, T., Cremers, S., et al., 2015. Treatment of obese insulin-resistant mice with an allosteric MAPKAPK2/3 inhibitor lowers blood glucose and improves insulin sensitivity. Diabetes 64(10):3396–3405.

[15] Kreusser, M.M., Lehmann, L.H., Keranov, S., Hoting, M.O., Oehl, U., Kohlhaas, M., et al., 2014. Cardiac CaM Kinase II genes delta and gamma contribute to adverse remodeling but redundantly inhibit calcineurin-induced myocardial hypertrophy. Circulation 130(15):1262–1273.

[16] Weinreuter, M., Kreusser, M.M., Beckendorf, J., Schreiter, F.C., Leuschner, F., Lehmann, L.H., et al., 2014. CaM Kinase II mediates maladaptive post-infarct remodeling and pro-inflammatory chemoattractant signaling but not acute myocardial ischemia/reperfusion injury. EMBO Molecular Medicine 6(10):1231–1245.

[17] Mather, K., 2009. Surrogate measures of insulin resistance: of rats, mice, and men. American Journal of Physiology. Endocrinology and Metabolism 296(2):E398–E399.

[18] Matthews, D.R., Hosker, J.P., Rudenski, A.S., Naylor, B.A., Treacher, D.F., Turner, R.C., 1985. Homeostasis model assessment: insulin resistance and beta-cell function from fasting plasma glucose and insulin concentrations in man. Diabetologia 28(7):412–419.

[19] Pfleiderer, P.J., Lu, K.K., Crow, M.T., Keller, R.S., Singer, H.A., 2004. Modulation of vascular smooth muscle cell migration by calcium/calmodulin-dependent protein kinase II-delta 2. American Journal of Physiology - Cell Physiology 286(6):C1238–C1245.

[20] Petersen, M.C., Madiraju, A.K., Gassaway, B.M., Marcel, M., Nasiri, A.R., Butrico, G., et al., 2016. Insulin receptor Thr1160 phosphorylation mediates lipid-induced hepatic insulin resistance. Journal of Clinical Investigation 126(11):4361–4371.

[21] Folch, J., Lees, M., Sloane Stanley, G.H., 1957. A simple method for the isolation and purification of total lipides from animal tissues. Journal of Biological Chemistry 226(1):497–509.

[22] Myers, J.B., Zaegel, V., Coultrap, S.J., Miller, A.P., Bayer, K.U., Reichow, S.L., 2017. The CaMKII holoenzyme structure in activation-competent conformations. Nature Communications 8:15742.

[23] Bhattacharyya, M., Karandur, D., Kuriyan, J., 2020. Structural insights into the regulation of Ca(2+)/calmodulin-dependent protein kinase II (CaMKII). Cold Spring Harbor Perspectives in Biology 12(6).

[24] He, Y., Perry, B., Bi, M., Sun, H., Zhao, T., Li, Y., et al., 2013. Allosteric regulation of the calcium-sensing receptor in obese individuals. International Journal of Molecular Medicine 32(2):511–518.

[25] Sassmann, A., Offermanns, S., Wettschureck, N., 2010. Tamoxifen-inducible Cre-mediated recombination in adipocytes. Genesis 48(10):618–625.

[26] Ye, R., Wang, Q.A., Tao, C., Vishvanath, L., Shao, M., McDonald, J.G., et al., 2015. Impact of tamoxifen on adipocyte lineage tracing: inducer of adipogenesis and prolonged nuclear translocation of Cre recombinase. Molecular Metabolism 4(11):771–778.

[27] Eguchi, J., Wang, X., Yu, S., Kershaw, E.E., Chiu, P.C., Dushay, J., et al., 2011. Transcriptional control of adipose lipid handling by IRF4. Cell Metabolism 13(3):249–259.

[28] Wolins, N.E., Quaynor, B.K., Skinner, J.R., Tzekov, A., Park, C., Choi, K., et al., 2006. OP9 mouse stromal cells rapidly differentiate into adipocytes: characterization of a useful new model of adipogenesis. The Journal of Lipid Research 47(2):450–460.

[29] Valet, C., Batut, A., Vauclard, A., Dortignac, A., Bellio, M., Payrastre, B., et al., 2020. Adipocyte fatty acid transfer supports megakaryocyte maturation. Cell Reports 32(1):107875.

[30] Josephrajan, A., Hertzel, A.V., Bohm, E.K., McBurney, M.W., Imai, S.I., Mashek, D.G., et al., 2019. Unconventional secretion of adipocyte fatty acid

binding protein 4 is mediated by autophagic proteins in a sirtuin-1-dependent manner. Diabetes 68(9):1767–1777.

[31] Hunnicutt, J.W., Hardy, R.W., Williford, J., McDonald, J.M., 1994. Saturated fatty acid-induced insulin resistance in rat adipocytes. Diabetes 43(4):540–545.

[32] Dasgupta, S., Bhattacharya, S., Maitra, S., Pal, D., Majumdar, S.S., Datta, A., et al., 2011. Mechanism of lipid induced insulin resistance: activated PKCepsilon is a key regulator. Biochimica et Biophysica Acta 1812(4):495–506.

[33] Cho, Y.M., Kim, D.H., Lee, K.H., Jeong, S.W., Kwon, O.J., 2018. The IRE1alpha-XBP1s pathway promotes insulin-stimulated glucose uptake in adipocytes by increasing PPARgamma activity. Experimental & Molecular Medicine 50(8):102.

[34] Du, K., Herzig, S., Kulkarni, R.N., Montminy, M., 2003. TRB3: a tribbles homolog that inhibits Akt/PKB activation by insulin in liver. Science 300(5625):1574–1577.

[35] Freychet, P., Laudat, M.H., Laudat, P., Rosselin, G., Kahn, C.R., Gorden, P., et al., 1972. Impairment of insulin binding to the fat cell plasma membrane in the obese hyperglycemic mouse. FEBS Letters 25(2):339–342.

[36] Olefsky, J.M., 1976. Decreased insulin binding to adipocytes and circulating monocytes from obese subjects. Journal of Clinical Investigation 57(5):1165–1172.

[37] Zhou, L., Zhang, J., Fang, Q., Liu, M., Liu, X., Jia, W., et al., 2009. Autophagy-mediated insulin receptor down-regulation contributes to endoplasmic reticulum stress-induced insulin resistance. Molecular Pharmacology 76(3):596–603.

[38] Chen, Y., Huang, L., Qi, X., Chen, C., 2019. Insulin receptor trafficking: consequences for insulin sensitivity and diabetes. International Journal of Molecular Sciences 20(20).

[39] Goh, L.K., Sorkin, A., 2013. Endocytosis of receptor tyrosine kinases. Cold Spring Harbor Perspectives in Biology 5(5):a017459.

[40] Morcavallo, A., Genua, M., Palummo, A., Kletvikova, E., Jiracek, J., Brzozowski, A.M., et al., 2012. Insulin and insulin-like growth factor II differentially regulate endocytic sorting and stability of insulin receptor isoform A. Journal of Biological Chemistry 287(14):11422–11436.

[41] Cohen, A.W., Razani, B., Wang, X.B., Combs, T.P., Williams, T.M., Scherer, P.E., et al., 2003. Caveolin-1-deficient mice show insulin resistance and defective insulin receptor protein expression in adipose tissue. American Journal of Physiology - Cell Physiology 285(1):C222–C235.

[42] Saltiel, A.R., 2021. Insulin signaling in health and disease. Journal of Clinical Investigation 131(1).

[43] Zhang, W., Mottillo, E.P., Zhao, J., Gartung, A., VanHecke, G.C., Lee, J.F., et al., 2014. Adipocyte lipolysis-stimulated interleukin-6 production requires sphingosine kinase 1 activity. Journal of Biological Chemistry 289(46):32178–32185.

[44] Pereira, C., Schaer, D.J., Bachli, E.B., Kurrer, M.O., Schoedon, G., 2008. Wnt5A/CaMKII signaling contributes to the inflammatory response of macrophages and is a target for the antiinflammatory action of activated protein C and interleukin-10. Arteriosclerosis, Thrombosis, and Vascular Biology 28(3):504–510.

[45] Rusciano, M.R., Sommariva, E., Douin-Echinard, V., Ciccarelli, M., Poggio, P., Maione, A.S., 2019. CaMKII activity in the inflammatory response of cardiac diseases. International Journal of Molecular Sciences 20(18).

[46] Gao, M., Du, Y., Xie, J.W., Xue, J., Wang, Y.T., Qin, L., et al., 2018. Redox signal-mediated TRPM2 promotes Ang II-induced adipocyte insulin resistance via Ca(2+)-dependent CaMKII/JNK cascade. Metabolism 85:313–324.

[47] Timmins, J.M., Ozcan, L., Seimon, T.A., Li, G., Malagelada, C., Backs, J., et al., 2009. Calcium/calmodulin-dependent protein kinase II links ER stress with Fas and mitochondrial apoptosis pathways. Journal of Clinical Investigation 119(10):2925–2941.

[48] Xue, A., Wu, Y., Zhu, Z., Zhang, F., Kemper, K.E., Zheng, Z., et al., 2018. Genome-wide association analyses identify 143 risk variants and putative regulatory mechanisms for type 2 diabetes. Nature Communications 9(1):2941.

[49] Erickson, J.R., 2014. Mechanisms of CaMKII activation in the heart. Frontiers in Pharmacology 5:59.

[50] Guney, E., Arruda, A.P., Parlakgul, G., Cagampan, E., Min, N., Lee, Y., et al., 2020. Aberrant Ca2+ homeostasis in adipocytes links inflammation to metabolic dysregulation in obesity. bioRxiv. https://doi.org/10.1101/2020.10.28.360008.

[51] Yang, Y., Fu, M., Li, M.D., Zhang, K., Zhang, B., Wang, S., et al., 2020. O-GlcNAc transferase inhibits visceral fat lipolysis and promotes diet-induced obesity. Nature Communications 11(1):181.

[52] Hauck, A.K., Huang, Y., Hertzel, A.V., Bernlohr, D.A., 2019. Adipose oxidative stress and protein carbonylation. Journal of Biological Chemistry 294(4):1083–1088.

[53] Rudich, A., Tirosh, A., Potashnik, R., Hemi, R., Kanety, H., Bashan, N., 1998. Prolonged oxidative stress impairs insulin-induced GLUT4 translocation in 3T3-L1 adipocytes. Diabetes 47(10):1562–1569.

[54] Furukawa, S., Fujita, T., Shimabukuro, M., Iwaki, M., Yamada, Y., Nakajima, Y., et al., 2004. Increased oxidative stress in obesity and its impact on metabolic syndrome. Journal of Clinical Investigation 114(12):1752–1761.

[55] Straub, L.G., Efthymiou, V., Grandl, G., Balaz, M., Challa, T.D., Truscello, L., et al., 2019. Antioxidants protect against diabetes by improving glucose homeostasis in mouse models of inducible insulin resistance and obesity. Diabetologia 62(11):2094–2105.

[56] Wang, Q., Hernandez-Ochoa, E.O., Viswanathan, M.C., Blum, I.D., Do, D.C., Granger, J.M., et al., 2021. CaMKII oxidation is a critical performance/disease trade-off acquired at the dawn of vertebrate evolution. Nature Communications 12(1):3175.

[57] Wang, Y., Li, G., Goode, J., Paz, J.C., Ouyang, K., Screaton, R., et al., 2012. Inositol-1,4,5-trisphosphate receptor regulates hepatic gluconeogenesis in fasting and diabetes. Nature 485(7396):128–132.

[58] Beaudry, J.L., Kaur, K.D., Varin, E.M., Baggio, L.L., Cao, X., Mulvihill, E.E., et al., 2019. The brown adipose tissue glucagon receptor is functional but not essential for control of energy homeostasis in mice. Molecular Metabolism 22:37–48.

[59] Nielsen, T.S., Jessen, N., Jorgensen, J.O., Moller, N., Lund, S., 2014. Dissecting adipose tissue lipolysis: molecular regulation and implications for metabolic disease. Journal of Molecular Endocrinology 52(3):R199–R222.

[60] Shearin, A.L., Monks, B.R., Seale, P., Birnbaum, M.J., 2016. Lack of AKT in adipocytes causes severe lipodystrophy. Molecular Metabolism 5(7):472–479.

[61] Sakaguchi, M., Fujisaka, S., Cai, W., Winnay, J.N., Konishi, M., O'Neill, B.T., et al., 2017. Adipocyte dynamics and reversible metabolic syndrome in mice with an inducible adipocyte-specific deletion of the insulin receptor. Cell Metabolism 25(2):448–462.

[62] Morley, T.S., Xia, J.Y., Scherer, P.E., 2015. Selective enhancement of insulin sensitivity in the mature adipocyte is sufficient for systemic metabolic improvements. Nature Communications 6:7906.

[63] Guetg, N., Abdel Aziz, S., Holbro, N., Turecek, R., Rose, T., Seddik, R., et al., 2010. NMDA receptor-dependent GABAB receptor internalization via CaMKII phosphorylation of serine 867 in GABAB1. Proceedings of the National Academy of Sciences of the United States of America 107(31):13924–13929.

[64] Hall, C., Yu, H., Choi, E., 2020. Insulin receptor endocytosis in the pathophysiology of insulin resistance. Experimental & Molecular Medicine 52(6):911–920.

[65] Xu, H., Barnes, G.T., Yang, Q., Tan, G., Yang, D., Chou, C.J., et al., 2003. Chronic inflammation in fat plays a crucial role in the development of obesity-related insulin resistance. Journal of Clinical Investigation 112(12):1821–1830.

[66] You, T., Ryan, A.S., Nicklas, B.J., 2004. The metabolic syndrome in obese postmenopausal women: relationship to body composition, visceral fat, and inflammation. The Journal of Cinical Endocrinology and Metabolism 89(11): 5517–5522.

[67] Weisberg, S.P., McCann, D., Desai, M., Rosenbaum, M., Leibel, R.L., Ferrante Jr., A.W., 2003. Obesity is associated with macrophage accumulation in adipose tissue. Journal of Clinical Investigation 112(12):1796–1808.

[68] Hotamisligil, G.S., Shargill, N.S., Spiegelman, B.M., 1993. Adipose expression of tumor necrosis factor-alpha: direct role in obesity-linked insulin resistance. Science 259(5091):87–91.

[69] Pedersen, D.J., Guilherme, A., Danai, L.V., Heyda, L., Matevossian, A., Cohen, J., et al., 2015. A major role of insulin in promoting obesity-associated adipose tissue inflammation. Molecular Metabolism 4(7):507–518.

